Optimal Alarm Logic Design for Mass-Flow Networks

Chii-Shang Tsai
Dept. of Chemical Engineering, Far East College, Tainan, Taiwan, Republic of China

Chuei-Tin Chang
Dept. of Chemical Engineering, National Cheng Kung University, Tainan, Taiwan 70101, Republic of China

An optimal alarm-system design method, which takes full advantage of the inherent hardware and spatial redundancies in a mass-flow network, is proposed. In particular, systematic procedures are developed to identify independent measurement methods for the flow rate of any stream in the process and to synthesize corresponding alarm generation logic. To implement the suggested alarm strategy, the formulas for evaluating conditional probabilities of type I and II mistakes are also derived. The results of applying the proposed alarm system to the application example show that the approach taken in this work is effective in suppressing the latter mistakes. Further, this system is superior to any of the existing alarm techniques in the sense that it can be appropriately tailored to minimize the expected loss due to misjudgments in generating alarms.

Introduction

To maintain a competitive edge, the rationales of computer-integrated manufacturing (CIM) have been gradually accepted by the process industries in recent years (Madono and Umeda, 1994; Nahara, 1994). The prerequisite of any CIM-related activity, such as production planning, operation scheduling, and advanced control, is the accessibility of reliable on-line process data. Consequently, earlier studies are mainly concerned with the development of computation techniques that make use of redundant information to ensure consistency in the estimates of key variables and then evaluate the process performance for the just cited purposes (Mah et al., 1976; Stanley and Mah, 1977; Mah, 1981; Crowe et al., 1983; Crowe, 1986). Although accurate estimates can be produced with such data reconciliation and coaptation procedures, and satisfactory results have been reported in practical applications, no systematic methods are currently available for constructing alarm systems that fully exploit the insights gained in these researches.

Alarm generation is in fact a basic function of the protective system in any chemical process plant (Lees, 1980). The current practice in the industry is simply to compare measurement data of the variable of interest with a predetermined threshold value. The decision concerning whether or not to set off an alarm is then made accordingly. Naturally, all measurements are subject to errors, that is, the random and/or gross errors (Mah, 1990). The former are usually assumed to be independently and normally distributed with zero mean. The latter can often be attributed to nonrandom causes such as instrument bias and measuring-device malfunction. Consequently, two types of mistakes may be committed in the preceding decision-making process. First, spurious alarms may be produced due to measurement noises when the variations of the process variables are actually within acceptable limits (type I mistakes). Second, the system may fail to detect the existence of hazardous operating conditions, and thus no alarms are generated (type II mistakes).

Statistical process control (SPC) strategies are probably the most widely adopted choice for the purpose of fault monitoring (Badavas, 1993; Kramer and Mah, 1994). However, if SPC techniques such as Shewhart or CUSUM charts are used directly for the present problem, there are drawbacks that require special attention. Notice first that the intention for installing an alarm system is usually to protect the process against certain hazards. Prompt remedial actions must be taken if such emergency situations occur. It is unacceptable to detect the out-of-statistical-control states *after* several consecutive measurements have already been obtained. In other words, it is highly desirable to reach safety-related con-

Correspondence concerning this article should be addressed to C.-T. Chang.

clusions as soon as a new batch of on-line measurement data are available. Second, it should be noted that the control limits used in SPC are in the strict sense *not* the same as the threshold limits of alarm. The former limits are set for testing the hypothesis that the observed process measurement does not differ significantly from its desired target value. Thus, these limits must be determined according to the statistics of measurement data obtained during normal operation. On the other hand, the latter limits are imposed mainly on the basis of process considerations. Consequently, a process variable that is out of statistical control may or may not trigger the alarm.

Another common industrial practice to reduce the chance of misjudgment is to introduce *hardware redundancy* in the alarm system (Lees, 1980). Specifically, several independent sensors are installed to monitor the same process variable. Any inconsistency identified in the measurement data obtained from different sensors is usually resolved on the basis of operation experience or an arbitrarily chosen alarm logic. It should be noted that the implied objective of such a practice is to achieve a compromise between the conflicting emphases on decreasing type I and type II mistakes. Although the traditional way of using hardware redundancy is effective on a qualitative basis in this respect, there are still several deficiencies. In particular, the conventional alarm strategy utilizes only the informations obtained from the redundant sensors for measuring the process variable of interest. Thus, other useful informations embedded in the process system is neglected completely. Also, the alarm-generating logic is developed on an *ad-hoc* basis, and thus may not be cost optimal. This drawback can be significant in cases when the financial loss from misjudgment is large.

One possible way to improve the current operation is to make use of both the hardware redundancy and the *spatial redundancy* in the sensor network of any process plant (Ali and Narasimhan, 1993, 1995). Thus, the reconciled data, rather than the raw measurement data, are adopted in this study for alarm-generation purposes. There are several advantages in taking this approach. The most obvious one is that the variances of estimates are known to be smaller than those of raw data (Mah et al., 1976). In addition, a collection of effective gross-error-detection techniques have already been developed (e.g., Mah and Tamhane, 1982; Iordache et al., 1985; Serth and Heenan, 1986; Narasimhan and Mah, 1987; Crowe, 1989; Narasimhan, 1990; Mah, 1990; Tjoa and Biegler, 1991; Rollins and Roelfs, 1992). These detection methods can be used in conjunction with the proposed alarm strategy. It should be noted that the former methods can only identify faults that invalidate material and/or energy balances. There may be other events that can drive the variables of interest out of acceptable ranges, for example, fouling in heat exchangers, and partial blockage in pipelines and external disturbances. In these situations, the reconciled values can naturally be adopted as the reference in an alarm system.

However, all reconciled estimates are also subject to errors, and thus type I and II mistakes are still possible in generating alarms. In order to minimize the expected loss of misjudgments due to these two types of mistakes, a systematic method for synthesizing the optimal alarm logics has been developed in this research. Basically, the design techniques for trip systems (Inoue et al., 1982; Kohda et al., 1983) have been extended for this purpose. In addition, in order to implement the proposed logic synthesis method, the probabilities of false alarms and undetected failures must be estimated in advance. An on-line estimation procedure for these parameters was also developed in this work. Finally, it should be noted that the scope of the present article is limited to mass-flow networks for the sake of brevity. The problems concerning both mass and energy balances will be addressed in a future article.

Error Models

The interdependence of flow and inventory data in a process is most naturally expressed in terms of material balances. In order to explore the network characteristics of the process, it is convenient to represent the mass-flow networks with process graphs (Mah et al., 1976). Without loss of generality, let us assume that all arcs in the process graph are measured. This is reasonable due to the fact that, if some arcs are unmeasured, one can always merge the nodes connected by these arcs to produce a graph in which only the measured ones exist.

Let us further assume that there are n streams in the process and their respective mass-flow rates are represented as x_j^t and $j = 1, 2, \ldots, n$. Due to unknown disturbances, the true flow rates can be viewed as

$$x_j^t = x_j^d + \delta_j \qquad j = 1, 2, \ldots, n, \tag{1}$$

where x_j^d denotes the design value of the flow rate of the jth stream and δ_j is the corresponding deviation of the true flow rate from its design value. In this study, δ_j is a normally distributed random variable with *time-variant* mean. Specifically, its expected value is zero when the system is operated at normal steady state and otherwise when faults occur.

The measurement errors are related to the true flow rates according to the following equations:

$$x_j^{(i)} = x_j^t + e_j^{(i)} \qquad i = 1, 2, \ldots, m_j \qquad j = 1, 2, \ldots, n, \tag{2}$$

where $x_j^{(i)}$ represents the measurement value of the jth stream using sensor i, $e_j^{(i)}$ denotes the corresponding error, and m_j is the total number of independent sensors used to measure the flow rate of stream j. Since the measurement errors are in general much smaller than the deviation δ_j caused by abnormal disturbances, it is thus assumed in this work that the means of $e_j^{(i)}$ are negligible. Specifically, $e_j^{(i)}$ is treated as a normally distributed random variable with zero mean in this study. Also, if sensor biases develop during operation, we assume that they can always be identified with available detection schemes (e.g., Mah, 1990), and the corresponding data can be removed before the generation of alarms. Finally, it is reasonable to believe that the variances of the measurement errors can be acquired from the vendor or an analysis of the historical data.

In this work, the reconciled values of flow rates are used in alarm-generation decisions. Consequently, the estimation errors must also be analyzed thoroughly. Let us consider a modified version of the reconciliation equation:

$$\hat{x} = \bar{x} - QA^T(AQA^T)^{-1}A\bar{x}, \tag{3}$$

where A is the incidence matrix of the process graph, Q is the covariance matrix associated with $\bar{x}$, $\hat{x}$ and $\bar{x}$ are two vectors defined as

$$\hat{x} = [\hat{x}_1, \hat{x}_2, \ldots, \hat{x}_n]^T$$

$$\bar{x} = [\bar{x}_1, \bar{x}_2, \ldots, \bar{x}_n]^T$$

and $\hat{x}_j$ and $\bar{x}_j$ ($j=1, 2, \ldots, n$) denote, respectively, the reconciled flow rate of the jth stream and the corresponding estimated value based on the measurement data obtained from the independent sensors installed on stream j. Both the least-square estimates and arithmetic averages can be used here. In either case, these estimates can be written as

$$\bar{x}_j = \sum_{i=1}^{m_j} \bar{w}_{ji} x_j^{(i)} \qquad j=1, 2, \ldots, n, \tag{4}$$

where $\bar{w}_{ji}s$ are the weights and $\Sigma_i \bar{w}_{ji} = 1$. Thus the mean and variance of the estimate $\bar{x}_j$ can be determined with the statistical parameters of the raw data $x_j^{(i)}$ ($i=1, 2, \ldots, m_j$). If there is only one sensor on each of the streams in process, then Eq. 3 reduces to its original form.

Let us now consider the estimation error, that is

$$\hat{x} = x^t + d \tag{5}$$

$$\bar{x} = x^t + \bar{e}, \tag{6}$$

where

$$x^t = [x_1^t, x_2^t, \ldots, x_n^t]^T$$

$$d = [d_1, d_2, \ldots, d_n]^T$$

$$\bar{e} = [\bar{e}_1, \bar{e}_2, \ldots, \bar{e}_n]^T.$$

Substituting Eqs. 5 and 6 into Eq. 3 and making use of the material balance equation, that is,

$$Ax^t = 0, \tag{7}$$

one can produce the following result:

$$d = \bar{e} - QA^T(AQA^T)^{-1}A\bar{e} = [I - QA^T(AQA^T)^{-1}A]\bar{e}. \tag{8}$$

Also, from Eqs. 5 and 6, one can obtain

$$\bar{e}_j = \sum_{i=1}^{m_j} \bar{w}_{ji} e_j^{(i)} \qquad j=1, 2, \ldots, n. \tag{9}$$

Consequently, the error of every reconciled flow rate can be represented as a linear combination of the measurement errors of all sensors, that is,

$$d_k = \sum_{j=1}^{n} \sum_{i=1}^{m_j} \omega_{kji} e_j^{(i)} \qquad k=1, 2, \ldots, n, \tag{10}$$

where the coefficients ω_{kji} can be determined by substituting Eq. 9 into Eq. 8.

Threshold Limits

Among the n streams in the process, there may be l ($l \le n$) streams on which alarms are installed. Associated with each of these l arcs, an operational constraint must be satisfied. The constraint associated with one of the streams, say stream a, can be written as

$$x_a^t - L_a \ge 0 \tag{11a}$$

or

$$U_a - x_a^t \ge 0, \tag{11b}$$

where L_a and U_a denote, respectively, the lower and upper threshold limit of flow rate. Thus, the operational constraints can be expressed in a general form:

$$\mathcal{G}(x_a^t) \ge 0, \tag{11c}$$

where $\mathcal{G}$ is referred to a *performance function*.

Obviously, an alarm is set off as an indication of constraint violation. Since the true flow rate x_a^t can never be determined, one has to rely on the measurement data to evaluate the performance function. In other words, the values of an indicator function $\mathcal{G}^{(s)}$ must be computed. This function is defined as

$$\mathcal{G}^{(s)} = \mathcal{G}(x_a^{(s)}) \qquad s=1, 2, \ldots, M_a, \tag{12}$$

where $x_a^{(s)}$ denotes the measurement value of stream a obtained with the sth independent method, and M_a is the total number of the measurement methods. Due to measurement errors, the values of the indicator function evaluated with data obtained from different methods are in general not consistent with one another. Nonetheless, one is still required to make a decision concerning whether or not to set off an alarm with these data. In the industries, the alarm-generation logics are usually developed on an *ad hoc* basis using only hardware redundancy (Lees, 1980). For example, an alarm may be generated according to the most reliable on-line sensor or an arbitrarily chosen l_a-out-of-m_a ($l_a \le m_a$) logic, and so on. As mentioned before, the objective of our research is to construct optimal alarm systems according to on-line measurement data. Obviously, it is advantageous to incorporate *both* hardware and spatial redundancies in the same alarm logic. In other words, the number of independent measurement methods should be larger than that used in the current practice, that is, $M_a \ge m_a$. Therefore, let us turn our attention to the problem of identifying independent flow measurement methods in a mass-flow network next.

Identification of Independent Measurement Methods

Obviously, the m_a independent sensors installed on stream a can be used as a means of *directly* measuring the flow rate of stream a. According to Ali and Narasimhan (1995), all the different ways of *indirectly* determining the same mass flow are given by the cut-sets that contain stream a in which the mass flow of every other stream is measured. However, since some of the elements may appear in more than two of these cut-sets, the corresponding measurement methods are statistically dependent. Consequently, it is necessary to select out cut-sets that do not contain common arcs other than a. Following is a simple procedure developed in this study to identify a set of independent indirect measurement methods:

1. Let the original process graph be the *current digraph* and also $i=1$.
2. Find a cut-set $\boldsymbol{K}^{(i)}$ of the current digraph that contains arc a.
3. Merge the input and output nodes of every arc in $\boldsymbol{K}^{(i)}$ except those of arc a. Let the resulting graph be the *current digraph* and $i=i+1$.
4. Repeat steps 2 and 3 until arc a itself forms a loop.

The following example is prepared to facilitate understanding of this procedure.

Example. Let us consider the process graph presented in Figure 1. It is assumed in this example that all its arcs are measured and the flow rate of stream 5 is the variable of interest. The independent *indirect* measurement methods can be identified with the following steps:

- Step 1: $i=1$ and the current digraph is the original process graph presented in Figure 1.
- Step 2: $\boldsymbol{K}^{(1)}=\{5, 3, 4, 6, 7\}$.
- Step 3: $i=2$ and the current digraph becomes the one presented in Figure 2a.
- Step 2: $\boldsymbol{K}^{(2)}=\{5, 10, 11, 12, 13\}$
- Step 3: $i=3$ and the resulting current digraph is presented in Figure 2b. Since arc 5 itself forms a loop in this case, the procedure should be terminated.

It should be noted that the cut-sets $\boldsymbol{K}^{(i)}$ $(i=1, 2, \ldots)$ obtained with the preceding procedure may not be unique. This is because more than one cut-set can usually be found in any given graph. Conceivably, other candidate measurement methods can be identified if a different cut-set is adopted in step 2. It should also be apparent that the number of such sets is at least two if the number of nodes in the process graph is larger than or equal to three. Consequently, it is usually possible to identify at least three independent measurement methods for a variable of interest in an industrial process.

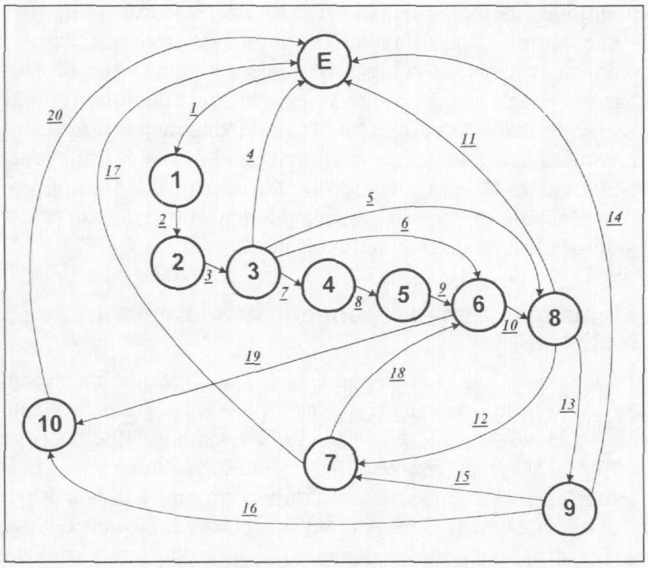

Figure 1. Process graph of a topping unit in refinery.

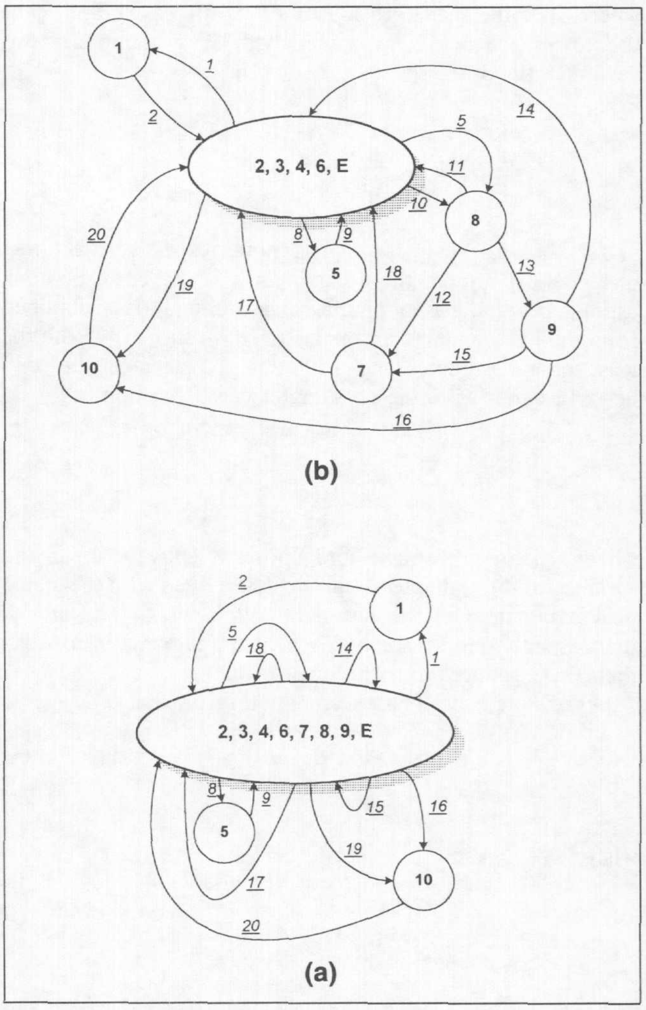

Figure 2. (a) Current digraph ($i=2$); (b) current digraph ($i=3$).

Synthesis of Optimal Alarm-generation Logic

As mentioned before, multiple measurement methods can be used to monitor the same variable of interest. Specifically, the on-line data are substituted into the performance function $\mathcal{G}$ to determine the current operation status. Let us assume that M_a measurement methods are chosen for this purpose. For illustration convenience, the labels of the sensors installed on stream a are stored separately in m_a different sets, that is,

$$S_s=\{j_a | j_a \text{ is the label of a sensor installed on stream } a\} \qquad s=1, 2, \ldots, m_a. \quad (13)$$

The labels of sensors used in the indirect measurement methods are also stored in another $M_a - m_a$ sets:

$$S_s=\{j_k | j_k \text{ is the label of a sensor on stream } k \text{ and } k \in K_a^{(s-m_a)}\}, \quad s=m_a+1, m_a+2, \ldots, M_a, \quad (14a)$$

in which

$$K_a^{(i)} = \{\eta | \eta \in K^{(i)} \quad \text{and} \quad \eta \neq a\}. \tag{14b}$$

Notice that each of the first m_a sets contains only one element, that is, the label of a sensor installed on stream a. The elements in the other $M_a - m_a$ sets are those included in $K_a^{(i)}$, which can be found with the proposed search procedure. For illustration purpose, the sets S_s are all collected in another sensor set $\mathcal{S}$. Corresponding to each $S_s \in \mathcal{S}$, a measurement value of the flow rate of stream a can be generated. If $s = 1, 2, \ldots, m_a$, this value is simply the measurement value obtained from the sth sensor installed on stream a. However, if $s > m_a$, the measurement value should be

$$x_a^{(s)} = \sum_k c_k^{(s)} x_k^{(j_k)} \qquad j_k \in S_s, \tag{15}$$

where k denotes an arc in process graph that is also a member of the set $K_a^{(s-m_a)}$, j_k is the label of a sensor selected in the sth measurement method for measuring the flow rate of stream k, and $c_k^{(s)}$ is the coefficient in the corresponding mass-balance equation used for determining the flow rate of stream a.

On the basis of these measurement values, a set of binary indicator variables y_s can be determined:

$$y_s = \begin{cases} 1 & \text{if } \mathcal{G}^{(s)} < 0 \\ 0 & \text{otherwise} \end{cases} \tag{16}$$
$$s = 1, 2, \ldots, M_a,$$

where $\mathcal{G}^{(s)}$ is the *indicator function* whose value can be determined by substituting the sth measurement values into the performance function.

The system alarm can then be generated on the basis of these indicators. The logic for setting off the alarm can be explicitly expressed with an alarm function $f(y)$, that is,

$$f(y) = \begin{cases} 1 & \text{if the system if generating an alarm} \\ 0 & \text{otherwise,} \end{cases} \tag{17}$$

where $y = [y_1, y_2, \ldots, y_{M_a}]^T$.

Obviously, the values of the indicator variables y_s may not be consistent with the true state x_a^t. Specifically, let us consider the true value of the performance function:

$$\mathcal{G}^t = \mathcal{G}(x_a^t). \tag{18}$$

There are two kinds of mistakes that can be identified accordingly—y_s is set to be 1 when $\mathcal{G}^t \geq 0$ (type I mistake) or y_s is set to be 0 when $\mathcal{G}^t < 0$ (type II mistake). Similarly, the mistakes committed in generating the *system alarm* can also be classified as type I and II. The conditional probabilities associated with these two mistakes—P_a and P_b—can be expressed as

$$P_a = Pr\{f(y) = 1 | \mathcal{G}^t \geq 0\} \tag{19}$$

$$P_b = Pr\{f(y) = 0 | \mathcal{G}^t < 0\}. \tag{20}$$

Since both types of mistakes result in financial losses, there are incentives for developing an optimal alarm-generating logic that minimizes the expected loss $\mathcal{L}$, that is,

$$\min_{f(y)} \mathcal{L}, \tag{21}$$

where

$$\mathcal{L} = C_a(1 - P_F)P_a + C_b P_F P_b, \tag{22}$$

where P_F is the demand probability, which is defined as the probability of violating the constraint, that is, $\mathcal{G}^t < 0$; C_a and C_b, respectively, denote the losses caused by type I and II mistakes in alarm generation. Notice that the conditional probabilities P_a and P_b can also be written as

$$P_a = \mathcal{E}[f(y) | \mathcal{G}^t \geq 0] = \sum_y f(y) Pr\{y | \mathcal{G}^t \geq 0\} \tag{23}$$

$$P_b = \mathcal{E}[1 - f(y) | \mathcal{G}^t < 0] = \sum_y [1 - f(y)] Pr\{y | \mathcal{G}^t < 0\}. \tag{24}$$

Thus, the expected loss becomes

$$\mathcal{L} = C_b P_F - \sum_y f(y) h(y), \tag{25}$$

where

$$h(y) = C_b P_F Pr\{y | \mathcal{G}^t < 0\} - C_a(1 - P_F) Pr\{y | \mathcal{G}^t \geq 0\}. \tag{26}$$

Notice that the first term on the righthand side of Eq. 25 represents the expected loss of the no-sensor system. Thus, it is apparent that the expected loss is minimized if the alarm function is chosen such that

$$f(y) = \begin{cases} 1 & \text{if } h(y) > 0 \\ 0 & \text{if } h(y) \leq 0. \end{cases} \tag{27}$$

After obtaining the values of $f(y)$ for all possible y, its functional form can be constructed accordingly. With the functional form given, the logic associated with $f(y)$ can be implemented as a hardwired circuit or as a computer program.

On-Line Probability Estimation

It should be noted that, in order to compute $h(y)$ and then construct $f(y)$, the estimates of demand probability and also conditional probabilities $Pr\{y | \mathcal{G}^t < 0\}$ and $Pr\{y | \mathcal{G}^t \geq 0\}$ must be obtained first. For illustration purpose, let us consider the constraint given in Eq. 11a. Using the relation presented in Eq. 1, the demand probability can be expressed as

$$P_F = Pr\{x_a^t < L_a\} = Pr\{\delta_a < L_a - x_a^d\}. \tag{28}$$

Since the mean of the deviation δ_a is time variant and thus unknown, it is not possible to evaluate P_F with Eq. 28. On the other hand, from the assumption of negligible $\mathcal{E}[e_j^{(i)}]$, the demand probability can be estimated according to the reconciled flow rate of stream a, that is,

$$P_F = Pr\{d_a > \hat{x}_a - L_a\}. \tag{29}$$

Notice that P_F must be computed on-line in this case. The parameters of the probability density function of d_a can be obtained according to Eq. 10, that is,

$$\mathcal{E}[d_a] = 0 \tag{30}$$

$$\text{Var}[d_a] = \sum_{j=1}^{n} \sum_{i=1}^{m_j} \omega_{aji}^2 \text{Var}\left[e_j^{(i)}\right]. \tag{31}$$

These parameters can be computed in advance. However, each time a new value of $\hat{x}_a$ is obtained with data-reconciliation techniques, the integration implied in Eq. 29 should be repeated.

The computation of the conditional probabilities can be simplified tremendously be taking advantage of the fact the measurement methods selected in $\mathcal{S}$ are s-independent. Specifically, they can be expressed as

$$Pr\{y | \mathcal{G}^t \geq 0\} = \prod_{s=1}^{M_a} a_s^{y_s}(1-a_s)^{1-y_s} \tag{32}$$

$$Pr\{y | \mathcal{G}^t < 0\} = \prod_{s=1}^{M_a} (1-b_s)^{y_s} b_s^{1-y_s}, \tag{33}$$

where

$$a_s = Pr\{y_s = 1 | \mathcal{G}^t \geq 0\} = Pr\{x_a^{(s)} < L_a | x_a^t \geq L_a\} \tag{34}$$

$$b_s = Pr\{y_s = 0 | \mathcal{G}^t < 0\} = Pr\{x_a^{(s)} \geq L_a | x_a^t < L_a\}. \tag{35}$$

From the definition of conditional probability, these two parameters can be written as

$$a_s = \frac{Pr\{x_a^{(s)} < L_a, x_a^t \geq L_a\}}{Pr\{x_a^t \geq L_a\}} \tag{36}$$

$$b_s = \frac{Pr\{x_a^{(s)} \geq L_a, x_a^t < L_a\}}{Pr\{x_a^t < L_a\}}. \tag{37}$$

Since the denominators in Eqs. 36 and 37 are simply $1 - P_F$ and P_F, it is only necessary to develop formulas for evaluating the numerators of these two parameters. Again, they are evaluated in this study according to the reconciled flow rate of stream a:

$$Pr\{x_a^{(s)} < L_a, x_a^t \geq L_a\} = Pr\left\{d_a - \epsilon_a^{(s)} > \hat{x}_a - L_a, d_a \leq \hat{x}_a - L_a\right\} \tag{38}$$

$$Pr\{x_a^{(s)} \geq L_a, x_a^t < L_a\} = Pr\left\{d_a - \epsilon_a^{(s)} \leq \hat{x}_a - L_a, d_a > \hat{x}_a - L_a\right\} \tag{39}$$

where

$$\epsilon_a^{(s)} = \begin{cases} e_a^{(s)} & s = 1, 2, \ldots, m_a \\ \sum_k c_k^{(s)} e_k^{(j_k)} \text{ and } j_k \in S_s & s = m_a+1, m_a+2, \ldots, M_a. \end{cases} \tag{40}$$

Notice that the expected values of $\epsilon_a^{(s)}$ are all zero. The parameters of the joint probability density function associated with the two random variables, $d_a - \epsilon_a^{(s)}$ and d_a, can be obtained from the means and variances of the measurement errors $\epsilon_j^{(i)}$ using Eqs. 10 and 40. As a result, it is always possible to evaluate the joint probabilities given in Eqs. 38 and 39 by numerical integration.

Application Example

Let us again consider Figure 1. This process graph is in fact the configuration of the topping unit in a refinery. Under normal operating conditions, it is assumed that the system is at its original steady state and can be described with the parameters presented in Table 1. The means and variances of true flow rates are listed, respectively, in the second and third columns. As mentioned previously, the mean of every deviation δ_j is considered to be zero during normal operation. Thus, the means $\mathcal{E}[x_j^t]$ in Table 1 are also used as the designed values x_j^d in the present example. In this topping unit, the flows of streams 3–7 and 10–13 are measured, and each with one sensor only. After merging the unmeasured arcs, the incidence matrix A becomes:

$$A = \begin{bmatrix} 1 & -1 & -1 & -1 & -1 & 0 & 0 & 0 & 0 \\ 0 & 0 & 1 & 0 & 0 & 1 & -1 & -1 & -1 \end{bmatrix}, \tag{41}$$

where the columns are associated with arcs 3–7 and 10–13, respectively, and the rows correspond to node 3 and node 8,

Table 1. System Parameters Under Normal Operating Conditions

Stream No. (j)	$\mathcal{E}[x_j^t]$	$\text{Var}[x_j^t]$	$\text{Var}[e_j]$	$\text{Var}[d_j]$
1	71,521.95	2,046,155.75	N.A.	N.A.
2	71,521.95	2,046,155.75	N.A.	N.A.
3	71,521.95	2,046,155.75	1,023,077.88	497,283.20
4	52,454.20	1,500,650.68	750,325.34	467,513.21
5	12,913.74	369,446.35	184,723.18	120,854.86
6	5,677.32	162,421.19	81,210.60	77,897.57
7	476.69	13,637.52	6,818.76	6,795.40
8	476.69	13,637.52	N.A.	N.A.
9	476.69	13,637.52	N.A.	N.A.
10	8,585.9	245,632.12	122,816.06	97,609.28
11	1,466.2	41,946.19	20,973.10	20,238.02
12	138.61	3,965.46	1,982.73	1,976.16
13	19,894.83	569,166.82	284,583.41	149,243.43
14	17,329.77	495,783.58	N.A.	N.A.
15	2,543.32	72,761.28	N.A.	N.A.
16	21.74	621.95	N.A.	N.A.
17	163.07	4,665.23	N.A.	N.A.
18	2,518.86	72,061.51	N.A.	N.A.
19	86.97	2,488.10	N.A.	N.A.
20	108.71	3,110.06	N.A.	N.A.

$$\begin{bmatrix} .4860 & .5139 & .3595 & .5139 & .5139 & -.1543 & .1543 & .1543 & .1543 \\ .3769 & .6230 & -.2637 & -.3769 & -.3769 & .1131 & -.1131 & -.1131 & -.1131 \\ .0649 & -.0649 & .6542 & -.0649 & -.0649 & -.2808 & .2808 & .2808 & .2808 \\ .0407 & -.0407 & -.0285 & .9592 & -.0407 & .0122 & -.0122 & -.0122 & -.0122 \\ .0034 & -.0034 & -.0023 & -.0034 & .9965 & .0010 & -.0010 & -.0010 & -.0010 \\ -.0185 & .0185 & -.1867 & .0185 & .0185 & .7947 & .2052 & .2052 & .2052 \\ .0031 & -.0031 & .0318 & -.0031 & -.0031 & .0350 & .9649 & -.0350 & -.0350 \\ .0002 & -.0002 & .0030 & -.0002 & -.0002 & .0033 & -.0033 & .9966 & -.0033 \\ .0429 & -.0429 & .4326 & -.0429 & -.0429 & .4755 & -.4755 & -.4755 & .5244 \end{bmatrix}$$

Figure 3. Matrix $I - QA^T(AQA^T)^{-1}A$.

respectively. Notice that all other nodes are merged into the environment node and thus the corresponding row is excluded from A. The variances of measurement errors are given in the fourth column of Table 1. If data reconciliation is performed according to Eq. 3, the variances of the estimation errors d_j can be computed with Eq. 8. The matrix $I - QA^T(AQA^T)^{-1}A$ used in this computation is presented in Figure 3 and the results are given in the fifth column of Table 1.

In the present example, it is again assumed that an alarm system must be installed on stream 5 to protect against the detrimental outcomes caused by low flow rate. The threshold limit L_5 selected in the simulation studies is 11,530.85 kg/h. The first independent measurement method is naturally associated with the sensor for directly measuring stream 5, that is, when $s = 1$

$$x_5^{(s)} = x_5^{(1)} = x_5, \tag{42}$$

where x_5 denotes the measurement data obtained with the sensor on stream 5. Notice that, since there is only one sensor on each stream in this case, the superscript of x_5 is dropped to simplify notation. The other independent measurement methods were identified with the proposed search procedure. Specifically, two cut-sets can be found—{5, 3, 4, 6, 7} and {5, 10, 11, 12, 13}. Thus, the indirect measurement methods can be expressed with the following material balance equations:

$$x_5^{(2)} = x_3 - x_4 - x_6 - x_7 \tag{43}$$

$$x_5^{(3)} = x_{11} + x_{12} + x_{13} - x_{10}. \tag{44}$$

In order to synthesize the optimal alarm logic on-line, one must be able to evaluate the conditional probabilities, a_s and b_s, with Eqs. 36 and 37. Consequently, the parameters in the probability density function (pdf) of d_5 and the joint pdfs of d_5 and $d_5 - \epsilon_5^{(s)}$ $(s = 1, 2, 3)$ should be determined in advance. These parameters can be determined with the data given in Table 1. In particular, the means were found to be zero, that is,

$$\mathcal{E}[d_5] = \mathcal{E}[d_5 - \epsilon_5^{(1)}] = \mathcal{E}[d_5 - \epsilon_5^{(2)}] = \mathcal{E}[d_5 - \epsilon_5^{(3)}] = 0. \tag{45}$$

Also, the variances and covariances needed for estimating the probabilities specified in Eqs. 38 and 39 were calculated to be:

$$\mathrm{Var}[d_5] = 120{,}854.89 \tag{46}$$

$$\mathrm{Var}[d_5 - \epsilon_5^{(1)}] = 62{,}806.86 \tag{47}$$

$$\mathrm{Var}[d_5 - \epsilon_5^{(2)}] = 1{,}726{,}844.10 \tag{48}$$

$$\mathrm{Var}[d_5 - \epsilon_5^{(3)}] = 315{,}592.82 \tag{49}$$

$$\mathrm{Cov}[d_5 - \epsilon_5^{(1)}, d_5] = -1{,}965.77 \tag{50}$$

$$\mathrm{Cov}[d_5 - \epsilon_5^{(2)}, d_5] = 1{,}680.24 \tag{51}$$

$$\mathrm{Cov}[d_5 - \epsilon_5^{(3)}, d_5] = 4{,}191.25. \tag{52}$$

The effectiveness of the proposed alarm-generating strategy can be demonstrated with simulation studies. The variation in flow rate x_5^t due to an unknown fault was first simulated. Initially, $\mathcal{E}[x_5^t]$ was kept at its designed value, 12,913.74 kg/h. The fault occurs at time $974\Delta t$, and Δt is the sampling interval. As a result, the mean flow rate of stream 5 decreases gradually and reaches a new steady level of 9,685.31 kg/h at time $1{,}074\Delta t$. The mean values of all other flow rates were generated in such a way that the constraint of the material balance is always maintained at every node in the process graph. The random-number generator RONNA in IMSL was used for producing the values of $(x_j^t - \mathcal{E}[x_j^t])$. The means of these random variables are zero and the variances are the same as $\mathrm{Var}[x_j^t]$ (see Table 1). Finally, the values of x_j^t were computed by adding $\mathcal{E}[x_j^t]$ and $(x_j^t - \mathcal{E}[x_j^t])$. A total of 2,000 sets of data have been generated in this case. Only half of them, that is, from sample 500 to 1,500, are shown in Figure 4.

Next, the measurement values x_j were simulated. This was done by adding the measurement errors e_j to the corresponding true flow rates x_j^t. The values of e_j were again created with a random-number generator. Using the measurement data, one can then compute the reconciled flow rates $\hat{x}_j$ with Eq. 3. A sample of the simulation results is presented in Figure 5. In this study, the traditional approach—using the raw measurement data of stream 5—was taken first to set off the alarm. The proportions of type I and II mistakes in this case were determined to be 0.05162 and 0.01321, respectively. On the other hand, by adopting the reconciled data as the basis for alarm generation, it was found that the chances of making these mistakes can be lowered significantly to 2.935% (type I) and 1.038% (type II).

Each time a new set of measurement data x_j and the corresponding reconciled flow rates $\hat{x}_j$ are obtained, an optimal

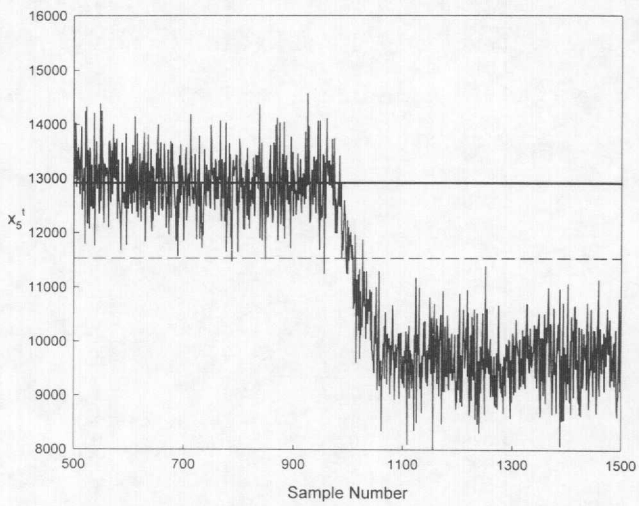

Figure 4. Simulation results of true flow rate x_5^t.

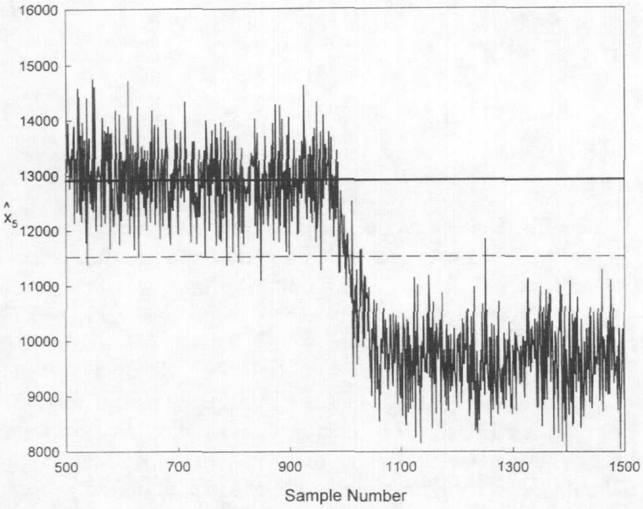

Figure 5. Simulation results of reconciled flow rate $\hat{x}_5$.

alarm logic can be constructed on-line with the proposed synthesis procedure. A sample of the alarm function $f(y)$ for the present example can be found in Table 2. The computation time needed to build one of these logics is about 2 s on a Pentium PC. To implement the implied alarm-generation strategy, values of $x_5^{(s)}$ $(s = 1, 2, 3)$ must also be determined with the three independent methods given in Eqs. 42–44.

Table 3. Performance of Optimal Alarm-generation Strategy

Alarm Strategies	C_b/C_a	Proportion of Mistake	
		Type I	Type II
Traditional	—	0.05162	0.01321
Approach A	—	0.02935	0.01038
Approach B	1.0	0.07389	0.00755
	3.0	0.13462	0.00189
	6.0	0.17611	0.00094
	9.0	0.20445	0.00000

These values are plotted in Figures 6a, 6b, and 6c, respectively. The results of adopting the proposed alarm policy (approach B) with different C_b/C_a ratios are summarized in Table 3. In particular, the proportions of types I and II mistakes are presented in this table. For purposes of comparison, the results of using only the direct-measurement data (the traditional approach) and the reconciled data (approach A) are also included. From these results, it is clear that the proposed method is superior in the sense that type II mistakes can be reduced to a negligible level. This is usually the first priority in most cases, since the purpose for installing an alarm is almost always to protect against certain catastrophic consequences. It should also be pointed out, however, that this improvement is often achieved at the expense of committing more type I mistakes. As the ratio C_b/C_a increases, the percentage of type I errors will inevitably increase also. This

Table 2. Values of Alarm Functions at Different Time Intervals

Sample No.	$f(0,0,0)$	$f(0,0,1)$	$f(0,1,0)$	$f(1,0,0)$	$f(0,1,1)$	$f(1,0,1)$	$f(1,1,0)$	$f(1,1,1)$
950	0	0	1	0	1	1	1	1
955	0	1	1	0	1	1	1	1
960	0	1	1	1	1	1	1	1
965	0	0	0	0	1	0	1	1
970	0	1	1	0	1	1	1	1
975	0	0	0	0	0	0	0	0
980	0	0	0	0	1	0	0	1
985	0	0	0	0	1	0	0	1
990	1	1	1	1	1	1	1	1
995	0	1	1	1	1	1	1	1
1,000	0	1	1	1	1	1	1	1
1,005	1	1	1	1	1	1	1	1
1,010	1	1	1	1	1	1	1	1
1,015	1	1	1	1	1	1	1	1
1,020	1	1	1	1	1	1	1	1
1,025	1	1	1	1	1	1	1	1
1,030	1	1	1	1	1	1	1	1
1,035	1	1	1	1	1	1	1	1
1,040	1	1	1	1	1	1	1	1
1,045	1	1	1	1	1	1	1	1
1,050	1	1	1	1	1	1	1	1
1,055	1	1	1	1	1	1	1	1
1,060	1	1	1	1	1	1	1	1
1,065	1	1	1	1	1	1	1	1
1,070	1	1	1	1	1	1	1	1
1,075	1	1	1	1	1	1	1	1
1,080	1	1	1	1	1	1	1	1
1,085	0	0	0	1	0	1	1	1
1,090	1	1	1	1	1	1	1	1
1,095	1	1	1	1	1	1	1	1
1,100	0	0	0	1	0	1	1	1

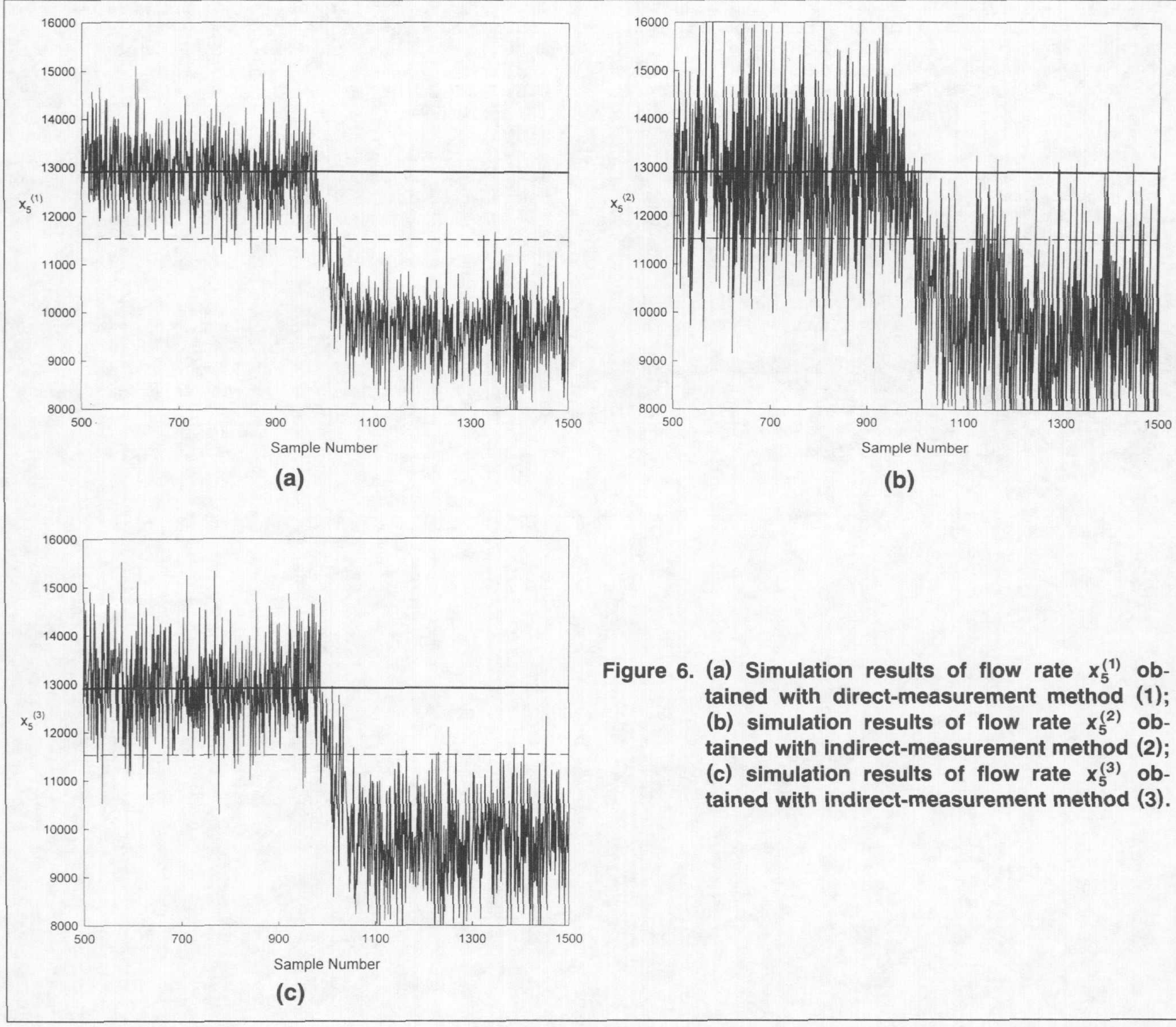

Figure 6. (a) Simulation results of flow rate $x_5^{(1)}$ obtained with direct-measurement method (1); (b) simulation results of flow rate $x_5^{(2)}$ obtained with indirect-measurement method (2); (c) simulation results of flow rate $x_5^{(3)}$ obtained with indirect-measurement method (3).

is nonetheless still acceptable as long as C_b/C_a is consistent with the primary design objectives.

Conclusions

From the preceding discussions, it is clear that the proposed alarm strategy is superior to any of the existing techniques. Such an improvement is brought about mainly by integrating two of the inherent features of mass-flow network, the hardware and spatial redundancies, into system design. This approach has never been attempted before. Furthermore, from experiences obtained in solving the example problem, one can also conclude that the demand for on-line computation is reasonable, especially when the sampling interval is in the range of minutes or longer.

Acknowledgment

This work was supported by the National Science Council of the ROC government under Grant NSC86-2214-E006-013.

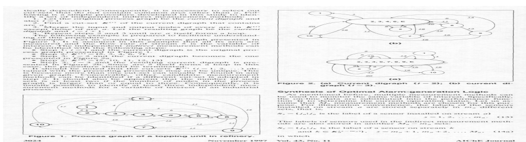

Literature Cited

Ali, Y., and S. Narasimhan, "Sensor Network Design for Maximizing Reliability of Linear Processes," *AIChE J.*, **39**, 820 (1993).

Ali, Y., and S. Narasimhan, "Redundant Sensor Network Design for Linear Processes," *AIChE J.*, **41**, 2237 (1995).

Badavas, P. C., *Real-Time Statistical Process Control*, Prentice-Hall, Englewood Cliffs, NJ (1993).

Crowe, C. M., Y. A. Garcia Campos, and A. Hrymak, "Reconciliation of Process Flow Rates by Matrix Projection: I. The Linear Case," *AIChE J.*, **29**, 881 (1983).

Crowe, C. M., "Reconciliation of Process Flow Rates by Matrix Projection: II. The Nonlinear Case," *AIChE J.*, **32**, 616 (1986).

Crowe, C. M., "Test of Maximum Power for Detection of Gross Errors in Process Constraints," *AIChE J.*, **35**, 869 (1989).

Inoue, K., T. Kohda, H. Kumamoto, and I. Takami, "Optimal Structures of Sensor Systems with Two Failure Modes," *IEEE Trans. Rel.*, **R-31**(4), 119 (1982).

Iordache, C. R., R. S. H. Mah, and A. C. Tamhane, "Performance Studies of the Measurement Tests for Detection of Gross Errors in Process Data," *AIChE J.*, **31**, 1187 (1985).

Kohda, T., H. Kumamoto, and K. Inoue, "Optimal Shut Down Logic for Protective Systems," *IEEE Trans. Rel.*, **R-32**(4), 26 (1983).

Kramer, M. A., and R. S. H. Mah, "Model-based Monitoring," *Foundations of Computer-Aided Process Engineering*, D. W. T. Rippin, J. C. Hale, and J. F. Davis, eds., CACHE, Austin, TX, p. 45 (1994).

Lees, F. P., *Loss Prevention in the Process Industries*, Vol. 1, Butterworth, London, p. 379 (1980).

Madono, H., and T. Umeda, "Outlook of Process CIM in Japanese Chemical Industries," *Foundations of Computer-Aided Process Engineering*, D. W. T. Rippin, J. C. Hale, and J. F. Davis, eds., CACHE, Austin, TX, p. 163 (1994).

Mah, R. S. H., G. M. Stanley, and D. M. Downing, "Reconciliation and Rectification of Process Flow and Inventory Data," *Ind. Eng. Chem. Proc. Des. Dev.*, **15**, 175 (1976).

Mah, R. S. H., "Design and Analysis of Process Performance Monitoring Systems," *Proc. Eng. Foundation Conf. on Chem. Process Control II*, Sea Island, GA (1981).

Mah, R. S. H., and A. C. Tamhane, "Detection of Gross Errors in Process Data," *AIChE J.*, **28**, 828 (1982).

Mah, R. S. H., *Chemical Process Structures and Information Flows*, Butterworth, Boston (1990).

Nahara, K., "Total Productive Management in the Refinery of the 21st Century," *Foundations of Computer-Aided Process Engineering*, D. W. T. Rippin, J. C. Hale, and J. F. Davis, eds., CACHE, Austin, TX, p. 111 (1994).

Narasimhan, S., and R. S. H. Mah, "Generalized Likelihood Ratio Method for Gross Error Determination," *AIChE J.*, **33**, 1514 (1987).

Narasimhan, S., "Maximum Power Tests for Gross Error Detection Using Likelihood Ratios," *AIChE J.*, **36**, 1589 (1990).

Rollins, D. K., and D. Roelfs, "Gross Error Detection with Constraints are Bilinear," *AIChE J.*, **38**, 1295 (1992).

Serth, R. W., and W. A. Heenan, "Gross Error Detection and Data Reconciliation in Steam-metering Systems," *AIChE J.*, **32**, 733 (1986).

Stanley, G. M., and R. S. H. Mah, "Estimation of Flows and Temperatures in Process Network," *AIChE J.*, **23**, 642 (1977).

Tjoa, I. B., and L. T. Biegler, "Simultaneous Strategies for Data Reconciliation and Gross Error Detection of Nonlinear Systems," *Comput. Chem. Eng.*, **15**, 679 (1991).

Manuscript received Dec. 26, 1996, and revision received July 7, 1997.